

UV Resonance Raman Spectra Reveal a Structural Basis for Diminished Proton and CO₂ Binding to α,α -Cross-Linked Hemoglobin[†]

Lisa A. Dick,[‡] George Heibel,[‡] Edwin G. Moore,[§] and Thomas G. Spiro^{*‡}

Chemistry Department, Princeton University, Princeton, New Jersey 08544, and Baxter Healthcare Corporation, 25212 West Route 120, Round Lake, Illinois 60073

Received July 21, 1998; Revised Manuscript Received November 24, 1998

ABSTRACT: UV resonance Raman difference spectra between ligated and deoxyhemoglobin contain tryptophan and tyrosine signals which arise from quaternary H-bonds in the T state, which are broken in the R state. These H-bonds are unaffected by bis(3,5-dibromosalicyl) fumarate cross-linking at the Lys α 99 residues, which prevents dissociation of Hb tetramers to dimers. However, when the pH is lowered from 9.0, or when NaCl is added, intensity is diminished for the tyrosine Y8 and tryptophan W3 bands of cross-linked deoxyHb, but not of native deoxyHb. This effect is attributed to weakening of tertiary H-bonds involving Tyr α 140 and Trp α 14, when the T state salt bridge between Val α 1 and Arg α 141 is formed via protonation of the terminal amino group and anion binding. The Tyr α 140–Val α 93 H-bond connects the Arg α 141-bearing H helix with the Lys α 99-bearing G helix. Weakening of the H-bond reflects a tension between the fumarate linker and the salt-bridge. This tension inhibits protonation of the Val α 1 amino terminus, thus accounting for the diminution of both proton [Bohr effect] and CO₂ binding in the T state as a result of cross-linking.

The development of human blood substitutes remains an important scientific and medical goal (1). The short storage life of whole blood from donors, the need to type blood before use in emergencies, and the transmission of blood-borne infections including AIDS are compelling reasons to find a blood replacement. As the oxygen-carrying component in blood, hemoglobin (Hb)¹ has been targeted as a potential blood substitute source. However, the usefulness of Hb is compromised by dissociation of the tetrameric molecules into dimers, when they are not encapsulated in red cells. Dimerization raises the oxygen affinity, and lowers cooperativity. In addition, the dimers are cleared by the kidneys, severely limiting the half-life in plasma. To overcome the dimerization problem, methods have been developed to chemically cross-link hemoglobin (2, 3) and increase the overall circulation time by 2–3-fold (4).

However, the cross-link generally alters the functional properties of Hb. If the tetramer is cross-linked while in its ligated form (R state), then it may be inhibited from conversion to the T state in the deoxy form, resulting in a molecule with high oxygen affinity and low cooperativity. This is undesirable because low affinity and high cooperativity are needed for efficient transfer of oxygen to the tissues. Consequently, cross-linkers have been sought which are selective for deoxyHb (T state). A particularly useful agent is bis(3,5-dibromosalicyl) fumarate which can connect the

ϵ -amino groups of the Lys α 99 residues across the $\alpha_1\alpha_2$ subunit interface when the tetramer is in the T state (deoxyHb) (5). The result is a preparation, $\alpha\alpha$ Hb, which has decreased oxygen affinity, and only slightly reduced cooperativity (6).

However, the influence of allosteric effectors (H⁺, Cl[−], DPG, IHP) is substantially diminished in $\alpha\alpha$ Hb (7), and binding of CO₂ is likewise diminished (8). CO₂ forms carbamino adducts with the terminal amino groups of Hb, and its binding to deoxyHb is an important mechanism for the transport of CO₂ from the tissues to the lungs. The observation of perturbations to the T state was surprising since the cross-linker is specifically adapted to the T state, and might have been expected to perturb the R state instead. Indeed, there is some R state perturbation as revealed by shifts in the iron–histidine vibrational frequency in $\alpha\alpha$ HbCO phototransients (9). However, the CO₂ inhibition is greater for the deoxy than the ligated form of $\alpha\alpha$ Hb (8).

The mechanism for these heterotropic effects of cross-linking has not been obvious, since the linked Lys α 99 residues are not directly involved in the binding of effector molecules. Moreover, the crystal structure of $\alpha\alpha$ Hb reveals minimal distortions relative to Hb (5). We now report UV resonance Raman (UVR) spectra which yield new insight into the mechanism. UVR spectra report on the environment of aromatic residues in proteins, and previous work has shown the Hb spectra to contain useful information about tertiary as well as quaternary H-bonds of tyrosine and tryptophan (10). The present results are consistent with the view that the fumarate cross-linker in $\alpha\alpha$ Hb weakens the salt-bridge between the α chain termini in the T state, thereby diminishing both proton and CO₂ binding. However, the strength of the quaternary contacts at the $\alpha_1\beta_2$ interface is unaffected.

[†] This work was supported by Baxter Healthcare Corp. and NIH Grant GM 25158 from the National Institute of General Medical Sciences.

^{*} To whom correspondence should be addressed.

[‡] Princeton University.

[§] Baxter Healthcare Corp.

¹ Abbreviations: Hb, hemoglobin; $\alpha\alpha$ Hb, hemoglobin cross-linked between Lys99 α 1 and Lys99 α 2; IHP, inositol hexaphosphate; DPG, 2,3-diphosphoglycerate; UVR, ultraviolet resonance Raman.

EXPERIMENTAL PROCEDURES

Sample Preparation. Cross-linked Hb (6) was exchanged into pH 6.5 or 7.3 (35 mM phosphate) or pH 9.0 (15 mM borate) buffer, by three rinse/centrifuge cycles using Centricon concentrators. Raman samples were 1.0 mM in heme and 0.2 M in NaClO₄, added as an internal intensity standard. Inositol hexaphosphate (IHP) was prepared in 35 mM phosphate, pH 6.5, with a final concentration in Raman samples of 2.5 mM. HbCO was prepared by purging the Raman sample with CO gas for approximately 10 min in an open tube. DeoxyHb was prepared by purging HbCO with N₂ gas under illumination from a tungsten-halogen lamp at 5 °C for 4 h.

UVRR Spectroscopy. An intra-cavity-doubled argon laser (Coherent, Innova 300 FreD) was used to generate 229 nm cw laser excitation. Typical laser powers at the sample were 0.35 mW. Sample tubes were spun around a stationary helical stirring wire (10) and cooled with a stream of cold nitrogen gas to ~20 °C. An f/1 parabolic mirror collected the scattered light from a 135° backscattering geometry. An f-matching lens focused this light onto the entrance slit (150 μm) of a 1.26 m single monochromator (Spex 1269). The acquisition time was 0.5–1 h per sample in order to obtain high-quality difference spectra. During the acquisition, HbCO samples were purged with CO gas, while deoxyHb samples were purged with N₂ gas.

Spectral intensities were normalized by adjusting the heights of the perchlorate internal standard band at 934 cm⁻¹ in the deoxyHb and HbCO spectra, prior to subtraction. Sample concentrations were measured by UV/vis absorption, and used to correct the scale factor. For example, if evaporation by the N₂ purge concentrated a sample to 1.05 mM, the UVRR intensity was multiplied by 1.0/1.05.

RESULTS AND DISCUSSION

Unaltered $\alpha_1\beta_2$ Interface. DeoxyHb minus HbCO difference spectra are compared for native Hb and $\alpha\alpha$ Hb in Figures 1 and 2. Band assignments to tyrosine (Y) and tryptophan (W) residues (11) are indicated. The difference spectra are dominated by signals arising from the Trp β 37 and Tyr α 42 residues at the $\alpha_1\beta_2$ interface (12). These residues are located in the two critical contact regions, the 'hinge' and the 'switch' (13), and their signals monitor the strength of the T state interactions. They weaken significantly when the T state is destabilized by chemical modification (14) or mutation (15).

Trp β 37 forms a quaternary H-bond with the carboxylate side chain of Asp α 94, which is broken in the R state. The H-bond red-shifts the Trp excitation profile and increases the Trp β 37 contribution to the Raman scattering (10). As a result, the deoxy-minus-CO tryptophan difference bands are dominated by Trp β 37 (12). This is seen most clearly for W3, which is at 1548 cm⁻¹ for Trp β 37, but at 1558 cm⁻¹ for the interior residues Trp α 14 and - β 15, because of differences in the dihedral angle about the bond connecting the indole ring to the C β atom (16). The difference intensity is exclusively at 1548 cm⁻¹. As seen in Figures 1 and 2, the Trp difference signals are unaffected by pH or by addition of the allosteric effector inositol hexaphosphate (IHP), either for native Hb or for $\alpha\alpha$ Hb. Even though H⁺ and IHP stabilize the T state (17,18), they do not affect the strength of the

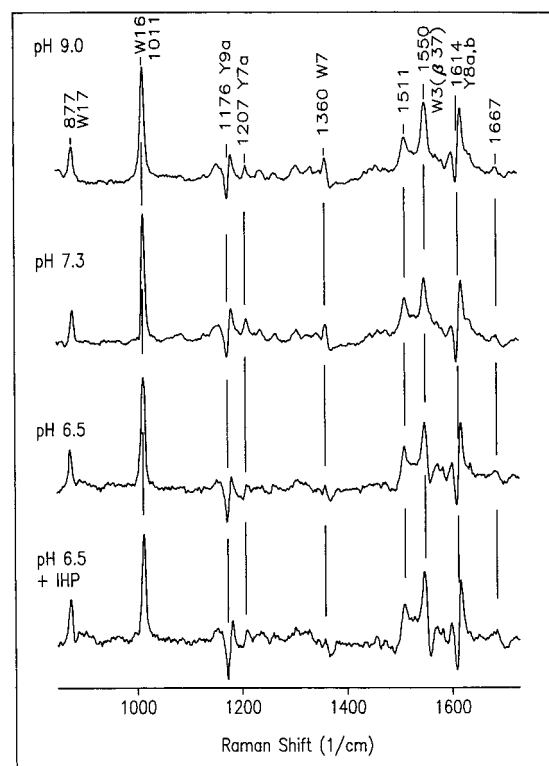


FIGURE 1: Native HbA (deoxy – CO) UVRR difference spectra as a function of pH and IHP. Experimental conditions: 1.0 mM heme, 0.2 M NaClO₄, 35 mM phosphate (pH 6.5 and 7.3), or 15 mM borate (pH 9.0); 0.35 mW, 229 nm laser excitation. From top to bottom: pH 9.0, pH 7.3, pH 6.5, and pH 6.5 + IHP.

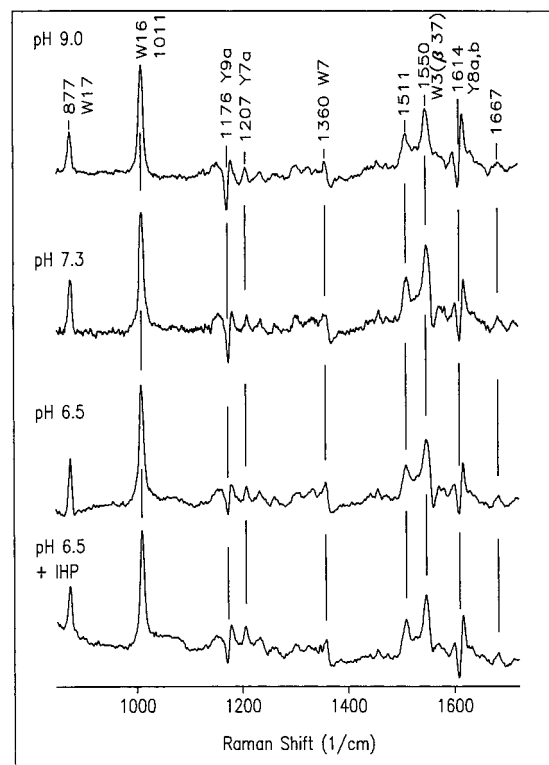


FIGURE 2: $\alpha\alpha$ Hb (deoxy – CO) UVRR difference spectra as a function of pH and IHP. Experimental conditions as in Figure 1. From top to bottom: pH 9.0, pH 7.3, pH 6.5, and pH 6.5 + IHP.

quaternary contacts at the 'hinge', which remain at full strength even at pH 9.0.

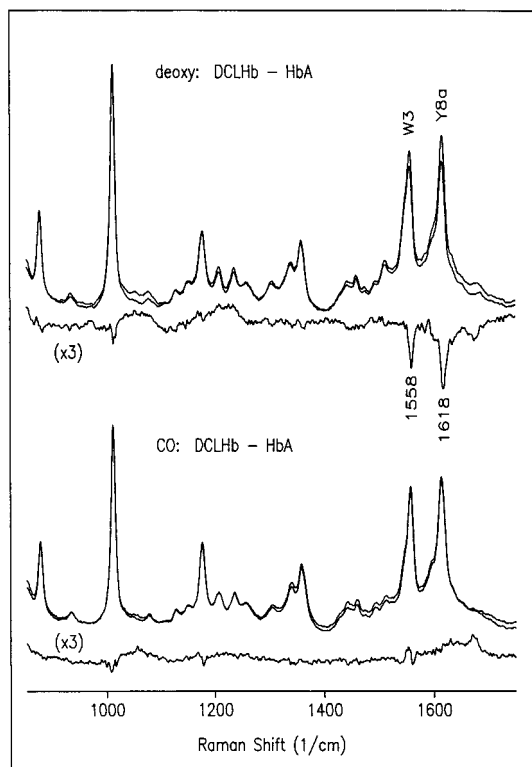


FIGURE 3: UVRR comparison of $\alpha\alpha$ Hb and native HbA in the CO and deoxy forms at pH 6.5. Experimental conditions as in Figure 1. Top, deoxy form; and bottom, CO form.

The same conclusion holds for the 'switch' contacts. Although tyrosine difference bands contain contributions from residues other than Tyr α 42, its quaternary H-bond with Asp β 99 is known to be responsible for the T state upshifts in Y8a,b bands, which are largely responsible for the sigmoidal difference features near 1600 cm^{-1} (12). This signal is unaffected by H^+ or IHP for native Hb.

Altered Tertiary H-Bonds. In the case of $\alpha\alpha$ Hb, the Y8a,b difference signal is as strong at pH 9.0 as it is for native Hb, but it diminishes somewhat as the pH is lowered (Figure 2). However, this diminution is not due to a change in the Y8a,b frequency upshifts, which remain unaltered. Rather it is due to a loss of Y8a intensity in deoxy- $\alpha\alpha$ Hb. This can be seen by subtracting the spectrum of deoxyHb from that of deoxy- $\alpha\alpha$ Hb (Figure 3). This difference spectrum contains a negative band at 1618 cm^{-1} , the position of Y8a. It also contains a negative band at 1558 cm^{-1} , the W3 position for the interior Trp residues, α 14 and β 15. On the other hand, the difference spectrum between the CO adducts of $\alpha\alpha$ Hb and native Hb contains only noise.

Thus, the UVRR spectra show that, even though the cross-linker is designed for the T state, it has no detectable effect on the R state, as reported by the aromatic residues, even though the Fe-histidine bond is known (9) to be influenced in the $\alpha\alpha$ HbCO photoproduct. But there is a T state effect on one or more tyrosine and tryptophan residues, resulting in intensity losses for W3 and Y8a. The intensity losses suggest H-bond weakening, but the quaternary H-bonds are unaffected, as reflected in the Trp β 37 and Tyr α 42 signatures. Instead, tertiary H-bonds must be weakened, consistent with the W3 position of the weakened intensity, which corresponds to Trp α 14 or - β 15.

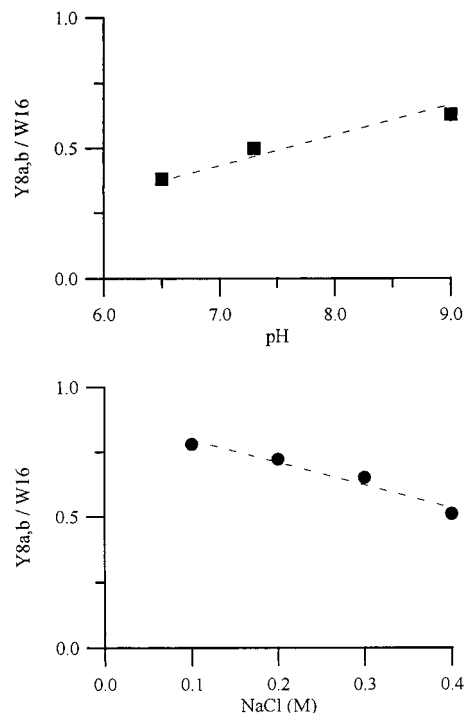


FIGURE 4: pH and Cl^- effects on the Y8a,b signal intensity for $\alpha\alpha$ Hb. Top graph: pH dependence of the Y8a,b signal in the presence of 0.2 M NaClO_4 . Bottom graph: NaCl dependence of the Y8a,b signal in 35 mM pH 7.3 phosphate buffer, 0.2 M NaClO_4 .

These interior Trp residues are located on the A helices of the two subunits, but form H-bonds with the OH side chains of Thr α 67 and Ser β 72, which are on the E helix, that lines the distal side of the heme pocket. The interior Trp residues give rise to negative UVRR signals when the HbCO spectrum is subtracted from spectra of tetramers having one or more deoxy-hemes, but which remain in the R state (R_{deoxy} spectra) (19–21). These signals are interpreted as arising from H-bond weakening due to E helix displacement toward the heme when ligands are absent in the R state.

Likewise, a weakened H-bond is the probable explanation of the negative W3 signal in $\alpha\alpha$ Hb. No doubt it is the Trp α 14 H-bond which is weakened since the cross-link connects residues in the α chains. For the same reason, weakening of an α chain tertiary H-bond from one of the Tyr residues is probably responsible for the negative Y8a signal.

We propose that this Tyr residue is Tyr α 140, which donates an H-bond to the backbone carbonyl of Val α 93 (Figure 4). This H-bond connects the G and H helices. The H helix is anchored by the salt-bridge between the carboxylate (α 1Arg141) and amine (α 2Val1) termini of the two α chains, while the G helix contains Lys α 99, the site of cross-linking. By drawing the two α chain G helices together, the cross-linker weakens the Tyr α 140–Val α 93 H-bond, which is restrained by the H helix anchor. Perturbation of the H helix can also account for the weakening of the Trp α 14–Thr α 67 H-bond, because the H helix buttresses the A helix (via interhelical H-bonds) (14), and can therefore control the A–E helix separation (19). It is known that removal of the Arg α 141 anchor results in a strengthening of the Trp α 14–Thr α 67 H-bond (14).

Bohr Effect and CO_2 Inhibition. This mechanism can account for the reduction in the Bohr effect and in CO_2

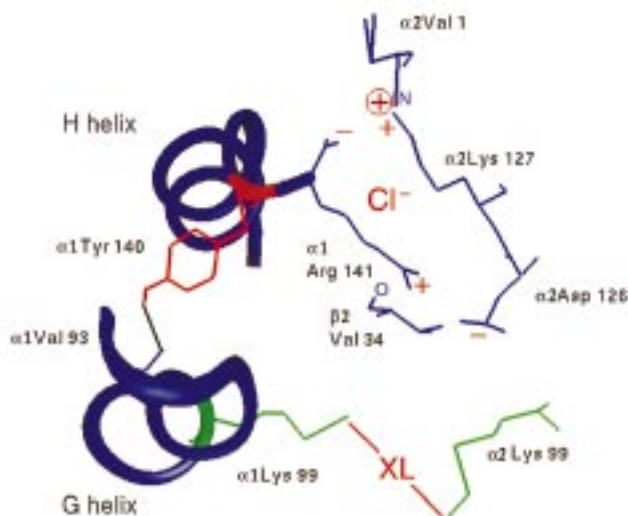


FIGURE 5: View of the α subunit G and H helices, showing the connection between the fumarate linker and the Val α 1 amino terminus, where protons and anions bind. [From crystallographic coordinates of deoxyHbA (29).]

Table 1: Peak Height of Trp and Tyr Difference Bands (Relative to 0.2 M Perchlorate) for Native Hb and $\alpha\alpha$ Hb

hemoglobin	W17	W16	Y9a	W3	Y8a,b
native Hb, pH 6.5–9.0	1.0	3.3	1.3	2.0	2.1
$\alpha\alpha$ Hb, pH 9.0	1.0	3.0	1.3	1.8	1.9
$\alpha\alpha$ Hb, pH 7.3	1.2	3.0	1.3	2.0	1.5
$\alpha\alpha$ Hb, pH 6.5	1.5	3.2	1.0	2.0	1.2
$\alpha\alpha$ Hb, pH 6.5, + IHP	1.2	3.4	1.3	1.8	1.7

binding of $\alpha\alpha$ Hb. The Val α 1 amino terminus is an important contributor of Bohr protons, since the T state salt-bridge requires protonation (22, 23). However, the cross-linking strains the salt-bridge (as evidenced by the H-bond weakening of both Tyr α 140 and Trp α 14), thereby inhibiting protonation. The cross-link-induced strain is apparent in the UVRR spectrum only as the pH is lowered from 9.0, suggesting a direct connection between amino protonation and weakening of the Tyr α 140 H-bond. As the pH is raised to 9.0, the Tyr α 140 H-bond is reestablished at full strength because the salt-bridge is weakened by Val α 1 deprotonation. The motions involved in this tug-of-war need not be more than a fraction of an angstrom, and might not be apparent in the X-ray crystal structure (5).

CO₂ binds to Hb by reacting with unprotonated terminal amine groups to form carbamino adducts (24). Thus, interference with Val α 1 protonation should enhance CO₂ binding. Instead, CO₂ binding is completely abolished in one of the chains in $\alpha\alpha$ Hb, and Vandegriff et al. argue that this abolition must occur in the α chains (8). They propose that the mechanism involves perturbation of the Arg α 14 side chain, whose positive charge stabilizes the anionic carbamino group. This suggestion is consistent with the present observations since perturbation of the salt bridge might well reposition the Arg α 141 side chain.

Anion Binding. Since cross-linking also inhibits chloride binding (7), we examined the effect of NaCl on the UVRR difference spectra. Indeed, addition of chloride has the same effect as lowering the pH (Figure 5), Table 1). The Y8a signal amplitude diminishes as NaCl is added to a pH 7.4 solution, just as it does when the pH is lowered to 6.5. This

observation is consistent with the idea that Cl[−] binds between the positive charges of the Val α 1 amino group and the Arg α 141 side chain (8). Bromide has been located at this position in the X-ray crystal structure of deoxyHb in solutions of poly(ethylene glycol) and 300 mM halide (25). However, the failure to see localized chloride electron density in a number of structures has led Perutz to propose that there is no specific chloride site; rather, chloride binds in the general region of the positively charged central cavity (26, 27). Two of these positive charges are on the Lys α 99 side chains, and are neutralized in the cross-linking reaction, thereby accounting for the 50% reduction in Cl[−] binding (7).

We find that chloride does not have the same effect as IHP on the UVRR spectrum. When IHP is added at pH 6.5 (Figure 2), the Y8a signal is partially restored. IHP also binds in the central cavity, but at a site located on the β chain side of the channel (28). Therefore, it would not participate directly in the balance of forces at the α chain termini. We propose that IHP restores the Tyr α 140 H-bond by neutralizing positive charge in the central cavity, and thereby releasing anions from the α chain side of the channel (the solutions without chloride contained 0.2 M NaClO₄ as internal standard). Thus, the α chain termini do provide binding sites for Cl[−], even if other sites are also available.

CONCLUSIONS

The UVRR spectra provide specific probes of aromatic residue interactions which permit us to conclude the following: (1) The critical $\alpha_1\beta_2$ quaternary interface is unaffected by fumarate cross-linking of the Lys α 99 residues. (2) Cross-linking does weaken tertiary H-bonds involving tyrosine and tryptophan residues.

These weakened H-bonds probably involve Tyr α 140 and Trp α 14. The Tyr α 140 H-bond bridges the cross-linked G helix with the H helix, which influences the Trp α 14 H-bond via H–A helix contacts. H helix perturbation also accounts for inhibition of proton, anion, and CO₂ binding to the Val α 1 amino terminus, which forms a salt bridge with the C-terminal Arg α 141, located at the end of the H helix.

REFERENCES

- Sanders, K. E., Ackers, G., and Sligar, S. (1996) *Curr. Opin. Struct. Biol.* 6, 534–540.
- Klotz, I., Haney, D. N., and King, L. C. (1981) *Science* 213, 724–731.
- Wood, L. E., Haney, D. N., Patel, J. R., Clare, S. E., Shi, G.-Y., King, L. C., and Klotz, I. M. (1981) *J. Biol. Chem.* 256, 7046–7052.
- Walder, R. Y., Andracki, M. E., and Walder, J. A. (1994) *Methods Enzymol.* 231, 274–280.
- Chatterjee, R., Welty, E. V., Walder, R. Y., Pruitt, S. L., Rogers, P. H., Arnone, A., and Walder, J. A. (1986) *J. Biol. Chem.* 261, 9929–9937.
- Snyder, S. R., Welty, E. V., Walder, R. Y., Williams, L. A., and Walder, J. A. (1987) *Proc. Natl. Acad. Sci. U.S.A.* 84, 7280–7284.
- Vandegriff, K., Medina, F., Marini, M. A., and Winslow, R. M. (1989) *J. Biol. Chem.* 264, 17824–17833.
- Vandegriff, K. D., Benazzi, L., Ripamonti, M., Perrella, M., Tellier, Y. C. L., Zegna, A., and Winslow, R. M. (1991) *J. Biol. Chem.* 266, 2697–2700.
- Larsen, R. W., Chavez, M. D., Ondrias, M. R., Courtney, S. H., Friedman, J. M., Lin, M. J., and Hirsch, R. E. (1990) *J. Biol. Chem.* 265, 4449–4454.

10. Rodgers, K. R., Su, C., Subramanian, S., and Spiro, T. G. (1992) *J. Am. Chem. Soc.* 114, 3697–3709.
11. Harada, I., and Takeuchi, H. (1986) in *Advances in Infrared and Raman Spectroscopy* (Clark, R. J. H., and Hester, R. E., Eds.) pp 113–173, John Wiley & Sons, New York.
12. Hu, X., and Spiro, T. G. (1997) *Biochemistry* 36, 15701–15712.
13. Baldwin, J., and Chothia, C. (1979) *J. Mol. Biol.* 129, 175–220.
14. Wang, D., and Spiro, T. G. (1998) *Biochemistry* 37, 9940–9951.
15. Hu, X., Mukherji, I., Rodgers, K. R., and Spiro, T. G. (1999) *Biochemistry*.
16. Miura, T., Takeuchi, H., and Harada, I. (1989) *J. Raman Spectrosc.* 20, 667.
17. Bohr, C., Hasselbalch, K., and Krogh, A. (1904) *Skand. Arch. Physiol.* 16, 402.
18. Marden, M. C., Bohn, B., Kister, J., and Poyart, C. (1990) *Biophys. J.* 57, 397–403.
19. Rodgers, K. R., and Spiro, T. G. (1994) *Science* 265, 1697–1699.
20. Jayaraman, V., Rodgers, K. R., Mukerji, I., and Spiro, T. G. (1995) *Science* 269, 1843–1848.
21. Mukerji, I., and Spiro, T. G. (1994) *Biochemistry* 33, 13132–13139.
22. Perutz, M. F. (1970) *Nature* 228, 726–734.
23. Garner, M. H., Richard, A., Bogart, J., and Gurd, F. R. N. (1975) *J. Biol. Chem.* 250, 4398–4404.
24. Kilmartin, J. V., Fogg, J., Luzzana, M., and Rossi-Bernardi, L. (1973) *J. Biol. Chem.* 248, 7039–7043.
25. Kavanaugh, J. S., Rogers, P. H., Case, D. A., and Arnone, A. (1992) *Biochemistry* 31, 4111–4121.
26. Perutz, M. F., Fermi, G., Poyart, G., Paganier, J., and Kister, J. (1993) *J. Mol. Biol.* 233, 536–545.
27. Perutz, M. F., Shih, D. T.-b., and Williamson, D. (1994) *J. Mol. Biol.* 239, 555–560.
28. Arnone, A., and Perutz, M. F. (1974) *Nature* 249, 34–36.
29. Fermi, G., Perutz, M. F., Shaanan, B., and Fourme, R. (1984) *J. Mol. Biol.* 175, 159–174.

BI981760D